

Impersonation Detection in AWGN-limited Underwater Acoustic Sensor Networks

Waqas Aman, Muhammad Mahboob Ur Rahman, Junaid Qadir

Electrical Engineering Department, Information Technology University (ITU), Lahore, Pakistan

{waqas.aman, mahboob.rahman, junaid.qadir}@itu.edu.pk

Abstract—This work addresses the problem of impersonation detection in an underwater acoustic sensor network (UWASN). We consider a UWASN consisting of M underwater sensor nodes randomly deployed according to uniform distribution within a vertical half-disc (the so-called trusted zone). The sensor nodes report their sensed data to a sink node on water surface on an additive white gaussian noise (AWGN) reporting channel in a time-division multiple-access (TDMA) fashion. The ongoing communication on the shared reporting channel is at risk of potential impersonation attack by an active-yet-invisible adversary (so-called Eve) present in the close vicinity, who aims to inject malicious data into the system. To this end, this work proposes a novel, two-step method at the sink node to thwart the potential impersonation attack by Eve. We assume that the sink node is equipped with a uniform linear array of hydrophones; and therefore, the estimates of the distance, angle of arrival, and the location of the transmit node are available at the sink node. The sink node exploits these measurements as device fingerprints to carry out a number of binary hypothesis tests (for impersonation attack detection) as well as a number of maximum likelihood hypothesis tests (for transmitter identification when no impersonation is detected). We provide closed-form expressions for the error probabilities (i.e., the performance) of most of the hypothesis tests. Furthermore, extensive simulation results (for various scenarios of Eve’s location) are provided, which attest to the efficacy of the proposed scheme.

I. INTRODUCTION

Underwater acoustic sensor networks (UWASN) are utilized by a multitude of civilian and military applications, e.g., sensing a specific area for resources, intrusion detection for border surveillance, and exploration of life underwater [1], [2]. In contrast to the terrestrial wireless networks, the UWASNs are exposed to the peculiar challenges of the underwater acoustic (UWA) channel, e.g. frequency-selective nature of path-loss and ambient noise, severe multipath (longer delay spreads), battery constraints, low (and variable) propagation speed of acoustic waves, and low data rates (for long-range communication) [1], [3]. The aforementioned challenges make the UWA channel quite error-prone, which calls for design of intelligent forward error correction (FEC) schemes, and retransmission schemes (e.g. ARQ) [3] tailored for UWASNs.

The broadcast nature of the acoustic channel also makes the UWASNs vulnerable to various kinds of security breaches by any nearby malicious nodes. Traditionally, the broadcast channels (e.g., terrestrial wireless, underwater acoustic) were secured via cryptography-based solutions at higher layers, where mutual trust is established a priori by pre-distributing a set of shared secret keys among the network entities.

Recently there has been tremendous interest in complementing the crypto-based security mechanisms at the higher layers with the feature-based physical layer security mechanisms [4]. Physical-layer security schemes build upon the so-called features (derived from the propagation medium’s characteristics, or hardware imperfections) to use them as *virtual keys* to enforce an additional layer of security in the network [4], [5].

Various kinds of attacks by adversaries have been investigated in the literature—e.g., impersonation (or, intrusion) attacks, eavesdropping attacks, Sybil attacks, denial-of-service attacks, wormhole attacks, jamming attacks, man-in-the-middle attacks, and malicious relaying—and a detailed survey of these attacks can be seen in the recent survey articles [4], [6], [7]. Most importantly, each physical-layer security scheme, like its higher layer counterpart, could counter only certain attacks (and not all of them) while making certain a priori assumptions about Eve (e.g., how much computational and infrastructural resources are at the disposal of Eve), which if violated by Eve renders the scheme ineffective [4], [5].

This work considers a UWASN whereby a set of M sensor nodes reports its sensed data to the sink node in a TDMA fashion, while a malicious node Eve is present in the close vicinity. This work assumes an active Eve. When Eve actively transmits, it may either announce its presence by executing a jamming attack, or it may remain in stealth mode to execute an impersonation attack. This work assumes that Eve remains in stealth mode only. That is, Eve—being a clever impersonator and not a mere jammer—wants to deceive the sink node by assuring it that Eve is indeed a legitimate sensor node. This way, Eve could potentially inject malicious data into the system to corrupt the system’s data integrity.

Contributions. This work presents a novel two-step method to thwart an impersonation attack by Eve. As for the first step, the sink node simply measures the distance of the sender node from itself to determine whether it lies within a trusted zone of radius d_0 or not. During the second step, the sink node measures the angle of arrival (AoA), and with that the sender node’s position as well. The estimates of distance, AoA, and position are exploited as fingerprints of the transmit device, and each of them is passed on to a maximum likelihood test followed by a binary hypothesis test. The individual binary decisions—*impersonation* or *no impersonation*—of all the tests in the second step are fused together (and the fusion outcome is further fused with the binary decision from the first

step) to generate the ultimate binary decision. As a by-product, the proposed method also performs transmitter identification when no impersonation is detected in the system.

Section II summarizes the prior art on security in UWASNs. But, to the best of authors' knowledge, a systematic treatment of (network-level) impersonation attack detection is missing in existing literature on UWASNs.

Outline. The rest of this paper is organized as follows. Section II summarizes the selected related work. Section III presents the system model. Section IV proposes a novel two-step method to thwart the impersonation attacks by Eve, followed by extensive simulation results in section V. Section VI concludes this paper.

II. RELATED WORK

Security in UWASNs is a subject that has not yet received much attention by the researchers so far. There are a few review articles ([6], [7], [8]) and a vision paper [9] though which list various kinds of attacks which the malicious nodes could launch against the UWASNs, and provide their own take on design of futuristic secure UWASNs. The articles [6]–[9] all admit that the security needs of UWASNs have not been addressed to full extent, i.e., there are many kinds of potential attacks (e.g. impersonation attack) for which no prevention/counter mechanisms have been reported in the literature. Nevertheless, the prior art on security in UWASNs is briefly summarized below.

The works in [10], [11], [12] provide cryptographic solutions to address the security needs of UWASNs. The authors of [10] consider both eavesdropping attack and the impersonation attack by the malicious node(s), and counter them by pre-distributing to the UWASN members a group key (which sensor nodes use to broadcast their sensed data to the group members) and a session key (which the sensor nodes use to send data to the sink node), while the sink node does the key management (e.g., the key generation, key updating, etc.). In [11], the same authors extend a well-known network discovery protocol (where sensor nodes discover their neighbor to develop routing tables), the so-called FLOOD protocol, to protect the UWASN from the spoofing (impersonation) attacks and denial-of-service attacks by intruders during the network discovery phase. Specifically, the authors of [11] recommend that each UWASN node should be provided a link key table (a link key is the pairwise agreement/key between the two neighboring nodes). Moreover, the neighboring nodes form the clusters (a cluster is one collision domain) whereby all the cluster members share a cluster key to communicate with each other. Ateniese et al. [12] present various cryptographic solutions for message encryption and authentication, i.e., generation of (block cipher based) symmetric keys, and (elliptic curves based) asymmetric keys.

The works in [13], [14], [15] all consider jamming attacks on UWASNs by active (and aggressive) intruders. The authors of [13] propose to route the sensed data to the sink node(s) via multiple paths (the so-called restricted flooding), which makes

the system jamming-resilient. Zuba et al. [14] conduct real-time jamming experiments with commercial (Benthos) acoustic OFDM modems in Mansfield Hollow Lake (in Mansfield, CT, USA) to demonstrate that jamming attacks could easily lead to denial of service predicament in UWASNs. Xiao et al. [15] utilize the tools from game theory to formulate the hostile interaction between jammers and UWASN nodes as a jamming game; the authors provide closed-form expressions for the Nash equilibrium when all the underwater channels are known. For the dynamic/uncertain underwater environments (when channels are not known), Xiao et al. [15] utilizes a reinforcement learning-based power control scheme to prevent the jamming attacks.

The works in [16], [17] consider passive eavesdropping attacks by a malicious node Eve. In [16], authors consider a 2-D region (a disk) which consists of multiple UWASN nodes (and one Eve node) distributed according to a Poisson point process. The authors then utilize tools from stochastic geometry to compute the probability that the eavesdropper is able to intercept the communication ongoing within the network, and show that the probability of interception decreases as more and more legitimate nodes fall outside the critical region around the Eve. [17] considers a one-way, secure communication problem where a node Alice transmits to another node Bob (in the presence of an Eve node); Huang et al. [17] propose that the Bob node exploits the block transmissions nature and large propagation delays of the acoustic channel to send out a jamming signal which interferes with the Alice's signal received at Eve, thus maximizing the secrecy capacity of the acoustic channel.

The works in [18], [19] study the problem of shared secret keys generation between a legitimate node pair by exploiting the physical-layer characteristics of the acoustic channel. To this end, Liu et al. [18] exploit the amplitude (i.e., received signal strength) of (reciprocal) time-varying, multipath, acoustic channel as the source of common randomness, followed by a fuzzy information reconciliation system (to remove the inconsistencies between the keys generated by the two nodes). Huang et al. [19], on the other hand, exploit the channel frequency response of the acoustic channel to generate the shared secret keys. [20] proposes SenseVault, a three-tier authentication framework to systematically generate (and update) cryptographic hash-based secret keys to authenticate the inter-cluster and intra-cluster UWASN nodes.

In short, *to the best of authors' knowledge, the problem of impersonation detection in UWASNs has not been reported in the literature yet.* On a side note, many experimental works have been reported in the literature on wireless sensor networks which attempt to do border surveillance and intrusion detection by deploying sensor nodes either over-the-ground or underwater, along the border (see the survey article [21]). We note, however, that the works summarized in [21] address the problem of an aggressive intruder (who is not interested to hide itself), while this work considers the scenario of a clever impersonator who aims to inject false data into the system while staying undetected.

III. SYSTEM MODEL

We consider a UWASN comprising M legitimate underwater sensor nodes (the so-called Alice nodes $\{A_i\}_{i=1}^M$) which report their sensed data to a sink node on the water surface (see Fig. 1). The sensor nodes are deployed randomly (according to uniform distribution) on a vertical half-disc (the so-called trusted zone). All the nodes in the considered system model constitute one collision domain, i.e. the UWASN under consideration is a *single-hop system* whereby each sensor (Alice) node could send its sensed data *directly* to the sink node. The shared reporting channel is time-slotted; the sensor nodes access the reporting channel in a TDMA fashion (and thus, there are no collisions). The ongoing communication on the reporting channel is at risk of impersonation attack by a malicious node Eve present nearby. This work considers an attack scenario whereby the Eve is in active (but stealth) mode, i.e., Eve attempts to impersonate some sensor (Alice) node before the sink node so as to inject some malicious data into the system.

Furthermore, this work relies heavily upon the following assumptions:

- The shared reporting UWA channel is memoryless¹ (i.e., multipath is negligible) and AWGN².
- All the nodes (M legitimate nodes, the sink node as well as the impersonator Eve) are stationary.
- The sink node has the necessary hardware, i.e., a uniform linear array (ULA) of hydrophones, to measure the angle of arrival (AoA) of incident sound wave from a transmit node.
- The noisy estimates of the distance and AoA of the channel occupant are available at the sink node³.
- Eve faithfully follows the communication protocol dictated by the sink node (to be described in the next section) in order to stay undetected.

IV. IMPERSONATION DETECTION AND TRANSMITTER IDENTIFICATION

As explained earlier, impersonation detection is a systematic framework to verify (at the physical layer) the identity of the sender node so as to detect-then-reject the data coming from the (stealth) impersonator node in order to maintain data integrity of the system.

The proposed method consists of two steps, which work together to carry out impersonation detection and transmitter identification. The first (second) step works under the assumption that the Eve node is outside (inside) the so-called trusted

¹One example scenario of a memoryless channel is when the UWASN is deployed in deep waters, and the shared reporting channel has a small range-to-depth ratio (and thus a small range). Furthermore, the reporting channel is narrow-band (and thus low-rate), and vertical (and thus multipath reflections are negligible). This reporting channel then acts as a line-of-sight link which is noise-limited only [22], [23].

²That is, the colored noise inherent to the system has been transformed into white noise by means of a pre-whitening filter at the sink node [24].

³This work assumes that the distance is estimated using two-way ranging based localization schemes [25], [26], [27], while the work [28] (and other works by the same authors) describes various ways to estimate AoA.

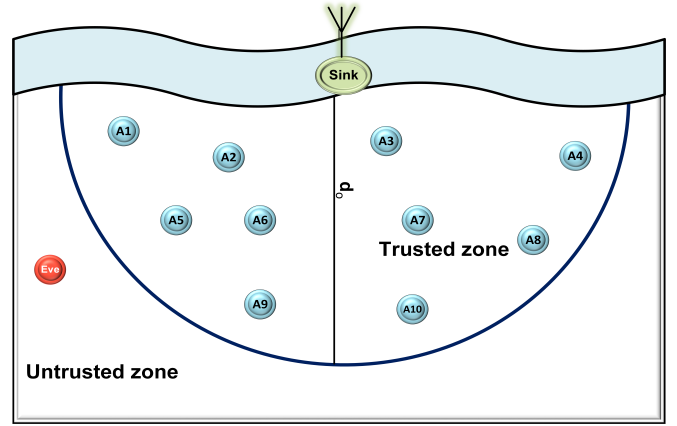


Fig. 1: An illustration of the system model using an example topology with $M = 10$ sensor nodes, and an Eve node.

zone. The first step consists of a distance bounding test, while the second step consists of three outlier detection tests.

A. Step 1: Distance-bounding test

This step is inspired by the proximity-based authentication techniques (which trust those transmit nodes only that are in the close proximity) in the radio-frequency identification systems [29], and the works on border intrusion detection [21]. This step assumes that Eve, being a clever impersonator, wants to remain undetected; therefore, it remains outside the trusted zone. As otherwise, if Eve enters the trusted zone, it might be detected by the system due to the on-board proximity sensors of the Alice node(s) [21].

The trusted zone. As a first layer of defense against the potential intrusion, the system relies upon the so-called trusted zone, a pre-defined geographic region around the sink node (i.e., a virtual fence). Specifically, this work considers a trusted zone which is a half-disc⁴ of radius d_0 when the sink node is placed at the origin (see Fig. 1). Under step 1, all the nodes inside the trusted zone (the half-disc) are considered to be legitimate nodes, while all the nodes outside the trusted zone are considered to be malicious/other nodes.

The distance-bounding protocol. Whenever the sink node receives some data on the shared reporting channel, it has to authenticate the sender of the data. As for the step 1, the sink node needs to estimate whether the sender node is inside the trusted zone or outside it. To this end, this work exploits the distance bounding protocol which works as follows. In the beginning of every time-slot, the sink node broadcasts a “challenge message” (see Fig. 2) which serves two purposes: i) it announces the beginning of the current time-slot to all the UWASN nodes, ii) it asks the channel claimant of the upcoming time-slot to prove its identity via transmission of a “response message”. This two-way communication constitutes the challenge-response based distance-bounding protocol [29].

⁴The trusted zone is a half-disc because under the distance bounding protocol, the sink node trusts the transmissions from the sender nodes which are less than d_0 distance away and vice versa.

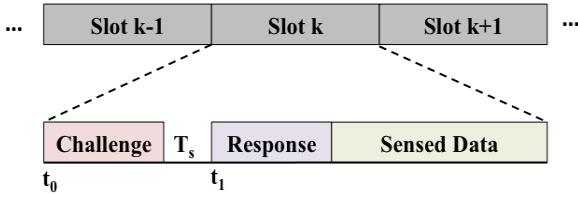


Fig. 2: Timeline of the TDMA reporting channel

Specifically, each challenge message from the sink node contains a (different) pseudo-noise (PN) sequence. The channel claimant node is required to echo back the PN sequence by putting it in its response message.

Distance estimation. Under distance-bounding protocol, the sink node needs to estimate the distance of the channel claimant from itself during every time-slot. To this end, the sink node marks the time instant t_0 of beginning of the challenge message; and a while later, estimates the time of arrival t_1 of the received response message via correlating the received noisy PN sequence against the stored copy of the same PN sequence. The sink node then computes an estimate of the round-trip time (RTT) as follows: $\hat{\Delta t} = \Delta t + T_s = t_1 - t_0$, where T_s is the so-called switching delay.⁵ With this, the sink node obtains the following distance estimate:

$$\hat{d} = v \frac{\hat{\Delta t}}{2} + n_d = v \frac{\Delta t}{2} + v \frac{T_s}{2} + n_d = d + v \frac{T_s}{2} + n_d \quad (1)$$

where $v = 1500$ m/sec is the (constant) speed of the acoustic waves under water; n_d is the estimation error: $n_d \sim N(0, \sigma_d^2)$. From Eq. (1), one can see that the sink node actually over-estimates the distance (because of the bias term $v \frac{T_s}{2}$). In this work, the sink node addresses this problem by pre-specifying a value for T_s (larger than the typical switching delays) which the channel claimant must abide by; then, the sink node obtains an unbiased distance estimate as follows: $z = \hat{d} - v \frac{T_s}{2}$.

Test 1: The distance bounding test. During the k -th time-slot, after computing the unbiased distance estimate $z(k)$, the sink node implements the test 1 as the following binary hypothesis test:

$$\begin{cases} H_0(\text{sender is in trusted zone}) : & z(k) = d_i + n_d(k) \\ H_1(\text{sender is in untrusted zone}) : & z(k) = d_E + n_d(k) \end{cases} \quad (2)$$

where d_i (d_E) is the distance of the A_i (Eve) node from the sink node. Since all the Alice nodes are deployed within the trusted zone, the binary hypothesis (BH) test in Eq. (2) translates to the following test:

$$z(k) \underset{H_0}{\overset{H_1}{\gtrless}} d_0 \quad (3)$$

The test 1 depicted in (3) approves the transmission from a sender node if the sender node is less than d_0 distance away from the sink node and vice versa.

⁵ T_s arises due to hardware limitations of a wireless/acoustic device to switch from receive mode to transmit mode.

Performance of the test 1. The BH test of (3) will incur two kinds of errors: false alarm (i.e., misclassifying some A_i as Eve), and missed detection (i.e., misclassifying Eve as some A_i). The probabilities for the both error events are as follows. The probability of false alarm is given as:

$$P_{fa} = \sum_{i=1}^M Pr(z(k) > d_0 | A_i) \pi(i) \quad (4)$$

where $z(k) | A_i \sim N(d_i, \sigma_d^2)$; $\pi(i)$ is the prior probability that the i -th Alice node A_i becomes the channel occupant during the k -th time-slot. This work considers the case of equal priors, i.e., $\pi(i) = \frac{1}{(M+1)}$. Then,

$$P_{fa} = \frac{1}{(M+1)} \sum_{i=1}^M Q\left(\frac{d_0 - d_i}{\sigma_d}\right) \quad (5)$$

where $Q(x) = \int_x^\infty \frac{e^{-\frac{t^2}{2}}}{\sqrt{2\pi}} dt$ is the standard Q -function.

Next, the probability of missed detection (the success rate of Eve) is given as:

$$P_{md} = Pr(z(k) < d_0 | E) \pi(E) \quad (6)$$

where $z(k) | E \sim N(d_E, \sigma_d^2)$; $\pi(E)$ is the prior probability that Eve node becomes the channel occupant during the k -th time-slot. Since P_{md} is a random variable (RV) (because d_E is an RV), we compute its expected value $\bar{P}_{md} := \mathbb{E}(P_{md})$ as follows:

$$\bar{P}_{md} = \frac{1}{(M+1)} \left(1 - \frac{1}{d_0(k-1) - \epsilon} \int_{d_0+\epsilon}^{kd_0} Q\left(\frac{d_0 - d_E}{\sigma_d}\right) dd_E \right) \quad (7)$$

where we have assumed that the unknown distance $d_E \sim U(d_0 + \epsilon, kd_0)$ where $\epsilon > 0$ is a small number and $k > 1$.

Remark 1. Despite its simplicity, the main strength of the distance-bounding protocol is that Eve (the malicious node) can not do any tampering to make \hat{d} appear lesser than d to the sink node. This is simply because Eve cannot tamper with the speed of acoustic waves under water. However, Eve could do the tampering to make \hat{d} appear greater than d by delaying the response message (beyond the value T_s suggested by the protocol, see Fig. 2). It is noted, however, that such tampering will not favor Eve, as the main intent of distance bounding protocol is to reject network access requests (and/or data) from the transmit nodes that are $> d_0$ distance away.

On the other hand, if Eve tries to send a response message (containing the malicious payload) before the challenge message is sent by the sink node, Eve will be detected due to two reasons: i) Eve's transmission could collide with the transmission of some (scheduled) Alice node from the previous slot; ii) Eve does not know the PN sequence the sink node has sent in its latest challenge message.

Remark 2. The RTT-based distance estimation under the distance bounding protocol is known as (two-way) ranging-based localization in the literature. We note that the two-way ranging-based localization schemes are (time) synchronization-free [25], [26], [27]. In other words, RTT

($\widehat{\Delta t} = t_1 - t_0$) estimation only requires two timestamps t_0 and t_1 generated by the local oscillator/clock of the sink node; therefore, no explicit time synchronization among the UWASN nodes is needed. Nevertheless, we emphasize that the periodic broadcast of the challenge message by the sink node implicitly enables (coarse) time synchronization in the network. This is because the UWASN nodes then follow a master-slave architecture where the sink node acts as master node, while the sensor nodes act as slave nodes.

B. Step 2: Outlier detection tests

This step addresses the scenario when the Eve node is potentially present within the trusted zone (e.g., because the on-board proximity sensors of the nearby Alice node(s) within the trusted zone were defunct). In such situation, step 1 fails to detect any impersonation attack. Therefore, the sink node implements the step 2, which utilizes AoA and position as additional device fingerprints. Then, for each of three fingerprints, the step 2 consists of an interplay between two kinds of sub-tests: a maximum likelihood (ML) hypothesis test followed by another BH test. As a by-product, the step 2 enables the sink node to perform transmitter identification (for the no impersonation case) as well.

AoA and Position as transmit device fingerprints. When the Eve is inside the trusted zone, the distance alone ceases to be effective as the fingerprint of the transmit node(s). This is because in this case $Pr(|d_i - d_E| < \eta) > 0$ for some i , $i = 1, \dots, M$ (η is a small number). Therefore, to resolve the situation when d_E is very similar to d_i (for some i), this step incorporates the angle of arrival as an additional fingerprint of the transmit device.

Let

$$y(k) = \hat{\theta}(k) = \theta + n_\theta(k) \quad (8)$$

where $y(k)$ represents the AoA measurement during the k -th time-slot; θ is the true AoA of the transmit node;⁶ $n_\theta(k) \sim N(0, \sigma_\theta^2)$ is the estimation error.⁷ Then, $\hat{p}(k) = z(k) \exp(jy(k))$ is the (derived) position estimate of the transmit node, obtained by the sink node during the k -th time-slot. In other words, this work performs a ranging-based source localization [27] and then the location estimate is used as fingerprint of the transmit device.

This work assumes that the positions of the legitimate nodes (a.k.a the ground truth) are known to the sink node in advance.⁸ In other words, $\mathbf{d} = \{d_1, \dots, d_M\}^T$, $\Theta = \{\theta_1, \dots, \theta_M\}^T$; and therefore, $\mathbf{p} = \{p_1, \dots, p_M\}^T$ (where $p_i = d_i \exp(j\theta_i)$) are available at the sink node. Then, under step 2, three tests are conducted, one for each device fingerprint. Furthermore, each test consists of an interplay between two sub-tests: an ML hypothesis test followed by another BH test.

⁶Assuming that the uniform linear array of hydrophones at the sink node is horizontally placed on the water surface (along the positive x-axis), the AoA is the angle made by a sensor node from positive x-axis in counter clockwise direction.

⁷ [28] describes various methods to estimate AoA in UWASNs.

⁸This is inline with the previous literature on impersonation attack detection at the physical layer [5], [30].

Test 2(a): Position based test. The ML sub-test works as follows:

$$i_p^* = \arg \max_{1 \leq i \leq M} f_{\hat{P}|A_i}(\hat{p}(k)) \quad (9)$$

where $f_{\hat{P}|A_i}$ is the probability density function (pdf) of $\hat{P}|A_i$. Essentially, the ML test returns the index i_p^* that maximizes the likelihood value $f_{\hat{P}|A_{i_p^*}}$, given the noisy observation $\hat{p}(k)$. However, we note that the closed-form expression for the pdf $f_{\hat{P}|A_i} \forall i$ is hard to derive. Therefore, we propose an alternative (sub-optimal) approach, the nearest-neighbour test. Let:

$$(J^*, i_p^*) = \min_i \|\hat{p}(k) - p_i\|_2 \quad (10)$$

Note that due to lack of prior knowledge about p_E (the position of Eve), the ML test only solves the transmitter identification problem (for Alice nodes, for the no impersonation case). For impersonation detection, one needs to define another binary hypothesis test which works as follows: if $\min_i \|\hat{p}(k) - p_i\|_2 > \epsilon_p$, then outlier/Eve is detected; else, the i -th Alice A_i from the ML test is declared to be the sender of the data (ϵ_p is a small threshold). Equivalently, the BH sub-test is:

$$\begin{cases} H_0(\text{no impersonation}) : & J^* = \min_i \|\hat{p}(k) - p_i\|_2 < \epsilon_p \\ H_1(\text{impersonation}) : & J^* = \min_i \|\hat{p}(k) - p_i\|_2 > \epsilon_p \end{cases} \quad (11)$$

The BH test in (11) can be re-written as:

$$J^* \underset{H_0}{\underset{H_1}{\geq}} \epsilon_p \quad (12)$$

The test in (12) approves the transmission from a sender node only if the position estimate $\hat{p}(k)$ of the sender node within the ball (around the point p_i) of radius ϵ_p and vice versa.

Test 2(b): Distance based test. The ML (equivalently, the nearest-neighbour) sub-test works as follows:

$$(K^*, i_d^*) = \min_i |z - d_i| \quad (13)$$

Next, the BH sub-test works as follows:

$$K^* \underset{H_0}{\underset{H_1}{\geq}} \epsilon_d \quad (14)$$

where ϵ_d is a small threshold, a design parameter.

Test 2(c): AoA based test. The ML sub-test works as follows:

$$(L^*, i_\theta^*) = \min_i |y - \theta_i| \quad (15)$$

Next, the BH sub-test works as follows:

$$L^* \underset{H_0}{\underset{H_1}{\geq}} \epsilon_\theta \quad (16)$$

where ϵ_θ is a small threshold, a design parameter.

Remark 3. The closed-form expressions for the two error probabilities (i.e., P_{fa} and P_{md}) could not be derived for the test 2(a) since the pdf of the test statistic J^* in Eq. (12) is not straightforward to obtain. However, the next subsection

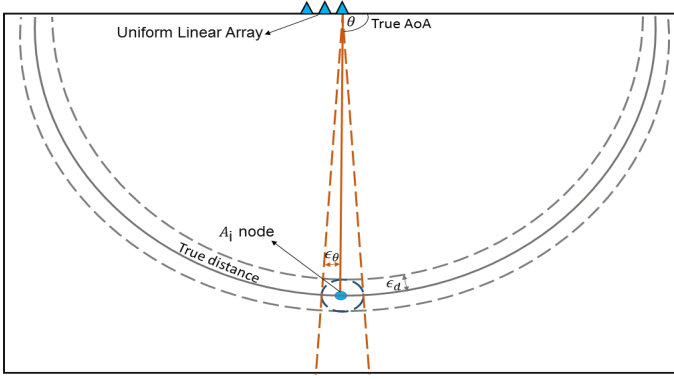


Fig. 3: The proximity regions of the three tests in step 2 (The sink node is shown to be equipped with a ULA containing three hydrophones.)

shares extensive simulation results which shed light on the performance of the tests 2(a), 2(b), 2(c) as well as the fusion rules (discussed below).

Performance of test 2(b). The two error probabilities for test 2(b) are:

$$\begin{aligned} P_{fa}^{(d)} &= P(K^* > \epsilon_d | H_0) \\ &= \frac{1}{(M+1)} \sum_{i=1}^M 2Q\left(\frac{\epsilon_d}{\sigma_d}\right) = \frac{2M}{(M+1)} Q\left(\frac{\epsilon_d}{\sigma_d}\right) \end{aligned} \quad (17)$$

and the expected value $\bar{P}_{md}^{(d)} := \mathbb{E}(P_{md}^{(d)})$ is as follows:

$$\begin{aligned} \bar{P}_{md}^{(d)} &= \mathbb{E}(P(K^* < \epsilon_d | H_1)) \\ &= \frac{1}{(M+1)(kd_0 - d_{min})} \\ &\quad \left(\int_{d_{min}}^{kd_0} \sum_{i=1}^M Q\left(\frac{d_i - \epsilon_d - d_E}{\sigma_d}\right) - Q\left(\frac{d_i + \epsilon_d - d_E}{\sigma_d}\right) dd_E \right) \end{aligned} \quad (18)$$

where we have assumed that the unknown distance $d_E \sim U(d_{min}, kd_0)$.

The expressions for $P_{fa}^{(\theta)}$ and $P_{md}^{(\theta)}$ for test 2(c) could be obtained in a similar way; and therefore, are omitted for the sake of brevity.

Remark 4. Each of the tests 2(a), 2(b) & 2(c) checks whether or not the noisy measurement of sender's fingerprint is within the so-called proximity region (PR) of any of the legitimate (Alice) nodes and decides accordingly. The PR, by definition, is a small region around the true value of each fingerprint, which represents the estimation errors. The PR is a half-ring (of width $2\epsilon_d$ meters) for the distance test, a cone (of width $2\epsilon_\theta$ degrees) for the AoA test, and a circle (of radius ϵ_p square meters) for the position test (see Fig. 3). As the next subsection will demonstrate, various levels of performance could be obtained by varying the size of the PR (or, equivalently, by varying the comparison thresholds ϵ_p , ϵ_d & ϵ_θ).

C. Impersonation detection

To detect the potential impersonation, first the individual binary decisions—*impersonation* or *no impersonation*—of all the three tests in the second step are fused together. Then, the fusion outcome is further fused with the binary decision from the first step to generate the ultimate binary decision.

The decision fusion of tests 2(a), 2(b) and 2(c). The individual decisions of tests 2(a), 2(b), 2(c) are fused via i) AND rule, ii) OR rule, iii) majority voting (MV) rule. Specifically, the AND (OR) rule is pessimistic (optimistic), i.e., a sender node is authenticated only if all (any one out of) the three tests decide H_0 . The AND (OR) rule strives to minimize P_{md} (P_{fa}).

The decision fusion of step 1 and step 2. When Eve is inside the trusted zone, step 1 is not helpful; therefore, only the outcome of step 2 should count to decide about the potential impersonation. On the other hand, when Eve is outside the trusted zone, the outcome of step 1 is equally helpful. To take into account both situations, this work applies the (pessimistic) AND rule to fuse the individual decisions made by step 1 & step 2 (which minimizes the ultimate probability of missed detection even further).

D. Transmitter identification

When both steps (step 1 and step 2) declare H_0 , i.e., no impersonation, then $i^* = MV(i_p^*, i_d^*, i_\theta^*)$ works as the transmit identifier. In this situation, the probability of misclassification error is given as:

$$\Pr_e = \sum_{i=1}^M \Pr_{e|i} \pi(i) \quad (19)$$

where $\Pr_{e|i} = \Pr(\text{Sink decides } A_j | A_i \text{ was the sender})$. For the distance based test (test 2(b)), $\Pr_{e|i}$ is given as:

$$\Pr_{e|i}^{(d)} = 1 - \left(Q\left(\frac{\tilde{d}_{l,i} - \tilde{d}_i}{\sigma_d}\right) - Q\left(\frac{\tilde{d}_{u,i} - \tilde{d}_i}{\sigma_d}\right) \right) \quad (20)$$

where $\tilde{d}_{l,i} = \frac{\tilde{d}_{i-1} + \tilde{d}_i}{2}$, $\tilde{d}_{u,i} = \frac{\tilde{d}_i + \tilde{d}_{i+1}}{2}$. Additionally, $\tilde{\mathbf{d}} = \{\tilde{d}_1, \dots, \tilde{d}_M\} = \text{sort}(\mathbf{d})$ where $\text{sort}(\cdot)$ operation sorts a vector in an increasing order. For the boundary cases, e.g., $i = 1$, $i = M$, $\tilde{d}_{l,1} = d_{min}$, $\tilde{d}_{l,M} = d_0$ respectively.

A similar expression exists for the misclassification error $\Pr_{e|i}^{(\theta)}$ for the AoA-based test (test 2(c)) which is omitted for the sake of brevity.

The algorithmic implementation of the proposed method has been summarized in Algorithm 1, while Fig. 4 provides a graphical summary.

V. PERFORMANCE EVALUATION

In this section, we will start by initially describing our simulation setup, and will then describe our simulation results.

Algorithm 1: The proposed method for Impersonation detection & Transmitter identification

Input : $\hat{p}(k) = z(k) \exp(jy(k))$
Output : b, i^* // i^* is the index of the sender node;
 $b = 1$ ($b = 0$) implies (no) impersonation.

Parameters: $\mathbf{p}, \mathbf{d}, \Theta, d_0, \epsilon_p, \epsilon_d, \epsilon_\theta, k$

- 1 Step 1: Distance bounding test:
- 2 implement the BH test in Eq. (2) and return binary decision
- 3 Step 2: Outlier detection tests:
- 4 implement the ML tests in Eq. (10), Eq. (13), Eq. (15) to return J^*, K^*, L^* and i_p^*, i_d^*, i_θ^*
- 5 implement the BH tests in Eq. (12), Eq. (14), Eq. (16) to return binary decisions for each test
- 6 Fusion of tests in step 2:
- 7 apply AND, OR, MV rules to fuse the individual decisions by tests in Eq. (12), Eq. (14), Eq. (16)
- 8 Impersonation detection:
- 9 apply AND rule to fuse the binary decisions by step 1 and step 2
- 10 Transmitter identification:
- 11 apply MV rule on i_p^*, i_d^*, i_θ^* to return the index i^* when H_0 is decided

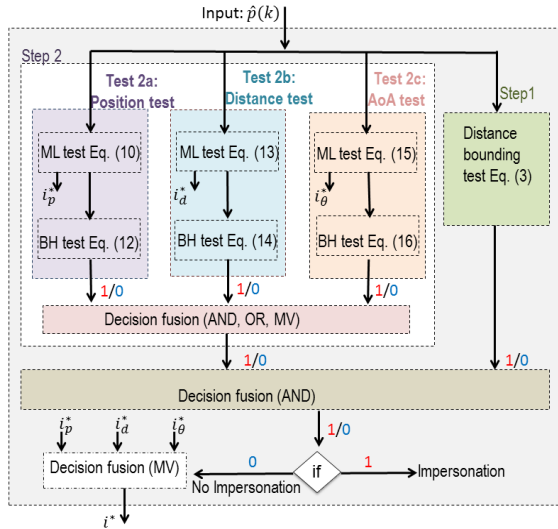
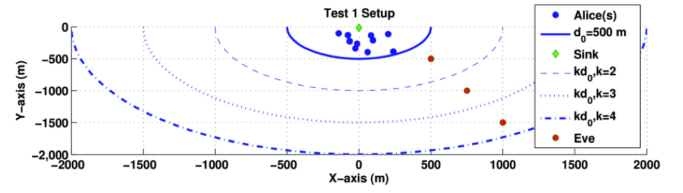


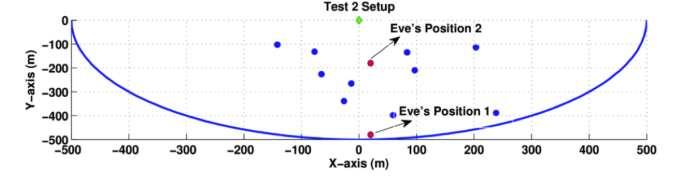
Fig. 4: The flow chart of the proposed method for Impersonation detection & Transmitter identification

A. Simulation Setup

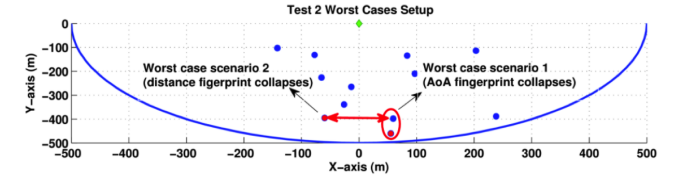
The performance evaluation was done in MATLAB. Fig. 5 shows the simulation setup. The sink node is placed at the water surface at (0,0), while a trusted zone, in the shape of a half-disc, of radius $d_0 = 500$ m is constructed around it. $M = 10$ Alice nodes are deployed according to uniform distribution within the trusted zone. One Eve node is present which is randomly placed either outside the trusted zone, or, inside it (see Fig. 5). The SNR at the sink node is defined as $1/\sigma^2$ where $\sigma^2 = \sigma_d^2 = \sigma_\theta^2 = \sigma_p^2$ is the common estimation error



(a) For *step 1*, the Eve node is randomly placed outside the trusted zone, but within one of three half-discs (of radius kd_0 where $k > 1$), one by one.



(b) For *step 2*, Eve is randomly placed at two different locations inside the trusted zone (where one location is close to, and other location is away from, the boundary of the trusted zone).



(c) To demonstrate the strength of position based test (the *test 2(c)*), two worst case scenarios are considered where Eve node is strategically placed at two locations which culminate in either distance, or, AoA ceasing to be effective as the fingerprint of the sender node.

Fig. 5: Simulation Setup

corrupting the measurements of distance, AoA and position at the sink node.⁹ Such simplistic definition of SNR allows us to compare the performance of the various hypothesis tests and fusion rules proposed in Algorithm 1 against each other.

B. Simulation Results

Fig. 6 plots the impersonation detection performance of step 1 (the distance bounding test). To obtain the results in Fig. 6, Eve is randomly placed at three different locations outside the trusted zone (see Fig. 5 (a)). Specifically, Fig. 6 sketches the tradeoff of the two error probabilities (P_{md}, P_{fa}) against the SNR whereby both P_{md} & P_{fa} decrease with an increase in SNR. However, since the centroid of the Alice nodes' positions (for the deployment shown in Fig. 5) is away from the boundary of the trusted zone, P_{fa} vanishes (to zero) much faster with an increase in SNR.

Figs. 7, 8, 9 together investigate the impersonation detection performance of step 2, while Fig. 10 investigates the transmitter identification performance of step 2.

⁹We assume that we have the mechanism to measure all the three features/fingerprints (i.e., distance, AoA and position) with same quality, for simplicity of exposition. Furthermore, SNR as defined here does not represent quality of the underwater acoustic reporting channel; it rather is an indicator of the quality of a measurement.

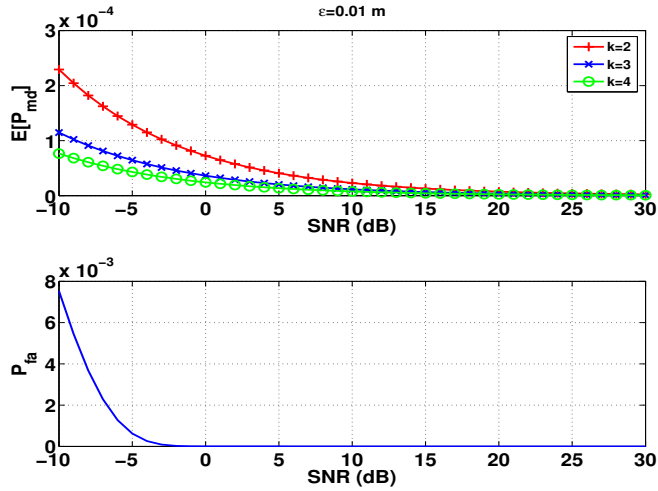


Fig. 6: Impersonation detection performance of *step 1*: Eve is placed outside the trusted zone (as depicted in Fig. 5 (a)). Both classification errors approach zero exponentially as the SNR is increased.

Fig. 7 studies the decay rate of the success probability of Eve (P_{md}) as a function of SNR. To obtain the results in Fig. 7, Eve is randomly placed at two different locations within the trusted zone (see Fig. 5 (b)). As anticipated, the AND (OR) rule being a pessimistic (optimistic) rule performs the best (worst). More precisely, for any given SNR, the AND (OR) rule minimizes (maximizes) the P_{md} ; equivalently, for any given requirement on P_{md} , the AND (OR) rule requires much lesser (higher) SNR compared to the other schemes. Additionally, the performance of the Position test is identical to that of AND rule (this is because the position/location, by definition, is the AND/combining of distance and AoA). Lastly, increasing the area of the proximity region for each of the tests 2(a), 2(b), 2(c) results in degradation of the detection performance of step 2.

Fig. 8 plots the probability of false alarm P_{fa} (an indicator of data rate shrinkage)¹⁰ as a function of SNR. Once again, the OR (AND) rule performs the best (worst) as anticipated. This is because the OR (AND) rule, by definition, minimizes (maximizes) the probability of false alarm. Furthermore, the performance of the Position test (test 2(a)) coincides with the performance of the AND rule. Finally, increasing the area of the proximity region for each of the tests 2(a), 2(b), 2(c) results in reduction in the probability of data rate shrinkage, as expected.

Fig. 9 captures the so-called worst case scenarios for test 2 whereby some individual (specifically, the weaker one) fingerprints collapse. Specifically, the first worst case scenario considers the situation where $|\theta_E - \theta_i| < \epsilon_\theta$ indefinitely

¹⁰False alarm, by definition, is the case when the sink node ends up discarding the data from the legitimate (Alice) nodes, which results in reduction in net data rate, increased latency due to re-transmissions, etc.

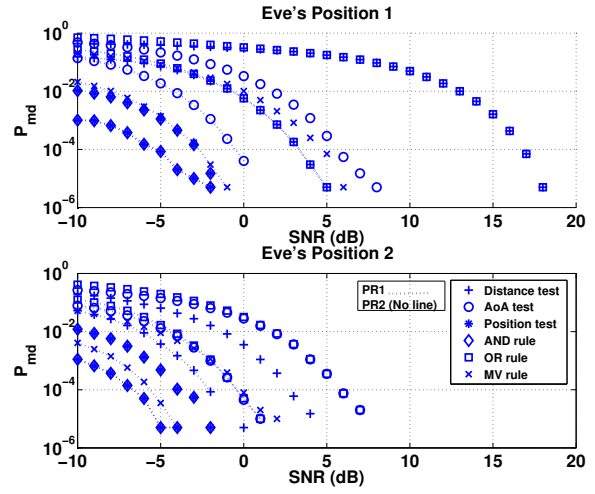


Fig. 7: Impersonation detection performance of *step 2*: Eve is placed at two locations inside the trusted zone (as depicted in Fig. 5 (b)); PR stands for proximity region; for PR1, $\epsilon_p = 1m^2$, $\epsilon_d = 1m$, $\epsilon_\theta = 1^\circ$; for PR2, $\epsilon_p = 3m^2$, $\epsilon_d = 3m$, $\epsilon_\theta = 3^\circ$. The success probability of Eve drops exponentially as the SNR is increased.

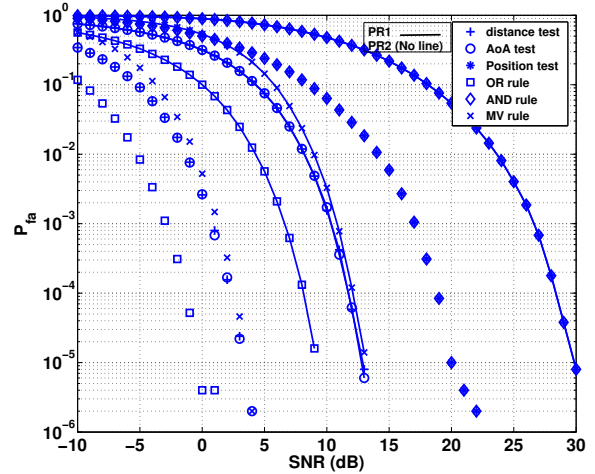


Fig. 8: Impersonation detection performance of *step 2*: Eve is placed inside the trusted zone; for PR1, $\epsilon_p = 1m^2$, $\epsilon_d = 1m$, $\epsilon_\theta = 1^\circ$; for PR2, $\epsilon_p = 3m^2$, $\epsilon_d = 3m$, $\epsilon_\theta = 3^\circ$. The false alarm rate vanishes to zero with an increase in the SNR.

(see Fig. 5 (c)). Therefore, in this situation, AoA ceases to be effective as the fingerprint of the transmit device. In such situation, SNR becomes a foe instead of a friend, i.e.,

$\lim_{SNR \rightarrow \infty} P_{md}^{(AoA)} = 1$ (see the top plot of Fig. 9). Similarly, the second worst case scenario captures the situation where $|d_E - d_i| < \epsilon_d$ indefinitely (see Fig. 5 (c)) which culminates in distance being ineffective as fingerprint of the transmit device.

Once again, an increase in SNR makes the situation worse, i.e., $\lim_{SNR \rightarrow \infty} P_{md}^{(d)} = 1$ (see the bottom plot in Fig. 9). However, one

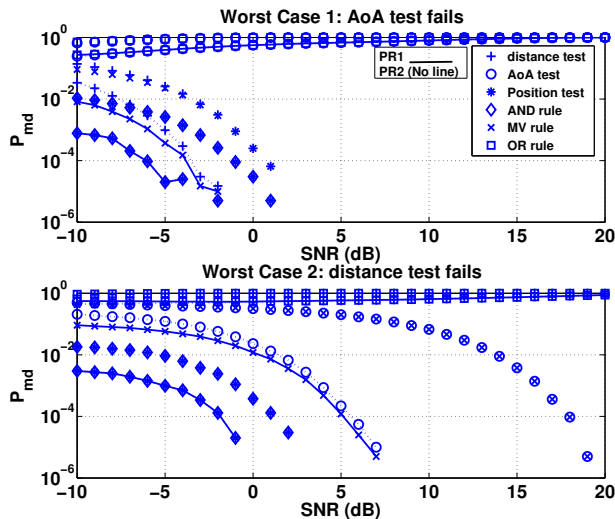


Fig. 9: Worst-case impersonation detection performance of *step 2*: Eve is strategically placed at two locations inside the trusted zone (as depicted in Fig. 5 (c)); for PR1, $\epsilon_p = 1 \text{ m}^2$, $\epsilon_d = 1 \text{ m}$, $\epsilon_\theta = 1^\circ$; for PR2, $\epsilon_p = 3 \text{ m}^2$, $\epsilon_d = 3 \text{ m}$, $\epsilon_\theta = 3^\circ$. For each of the two positions of Eve, either distance or AoA ceases to be effective as device fingerprint as its missed detection rate approaches one at high SNR values; however, location remains effective as fingerprint as its missed detection rate approaches zero at high SNRs.

can see that the Position test as well as AND rule gracefully sustain such worst case scenarios.¹¹

Fig. 10 plots the decay rate of the misclassification error P_{mc} (i.e., incorrectly identifying Alice i as Alice j) against SNR for all the three tests 2(a), 2(b), 2(c), and their fusion via MV rule. From Fig. 10, one can see that the Position test outperforms the other two tests (distance based, AoA based) by a big margin, while the curve for the MV rule is superimposed on the curve for the Position test. This is expected, because as explained in Remark 3, the proximity region of the Position test is much smaller than the proximity regions of the distance test and the AoA test.

C. Discussions

The results in Figs. 7, 8, 9 indicate that, under the impersonation detection problem, it is not possible to minimize both P_{md} and P_{fa} at the same time because of their conflicting nature. In other words, one could minimize one error type only by compromising on the other error type (which is inline with Neyman-Pearson Theorem [31]).

This work does not have experimental results to report to support the simulation results presented earlier. Nevertheless, the reader interested in experimental validation of the proposed impersonation detection framework is referred to the

¹¹The scenario $|p_E - p_i| < \epsilon_p$ is omitted simply because it implies that the Eve is co-located with some A_i (assuming that ϵ_p equals the size of a typical UWASN node).

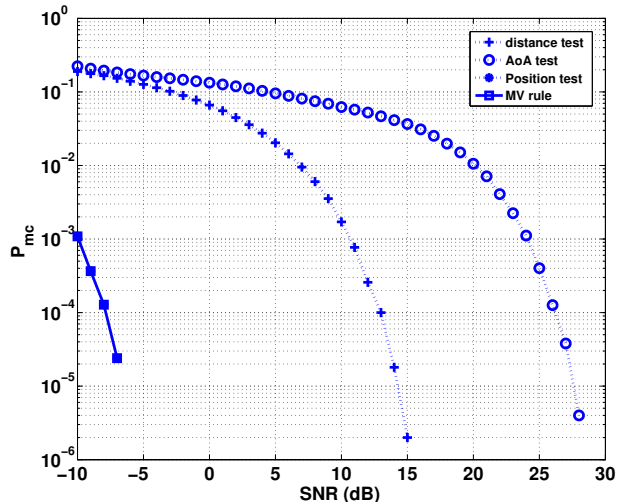


Fig. 10: Transmitter identification performance of *step 2*: The misclassification rate reduces to zero exponentially with increase in SNR. (The curve for the MV rule is superimposed on the curve for the position test).

works [32]–[34]. Specifically, [32] summarizes the state-of-the-art in commercial underwater acoustic modems, while the details pertinent to the (commercially available) arrays of hydrophones could be found in [33], [34] which report experimental results.

Though this work assumes a 2D geometry/deployment of the UWASN nodes for the sake of clarity of exposition, extension of the proposed impersonation detection framework to the case of 3D geometry/deployment of the UWASN nodes is laborious but straightforward. Yet, some comments are in order. Under the 3D geometry, the sink node will have to estimate two angles of arrival, the azimuth AoA θ and elevation AoA ϕ in addition to the distance estimation. For this purpose, the sink node could utilize a uniform circular array instead of a uniform linear array. With the distance estimate and the estimates of the two AoAs available, the sink node could then uniquely estimate the location/position of the transmit node as (d, θ, ϕ) in spherical coordinates. Furthermore, the additional angle of arrival could serve as an additional feature. But the overall framework (as summarized in Fig. 4 and Algorithm 1) remains the same as before.

VI. CONCLUSION & FUTURE WORK

This work addressed the problem of impersonation attack detection in a (white, Gaussian) noise-limited underwater acoustic sensor network. A novel, two-step method was proposed which utilized the distance, AoA, and location of a transmit device as device fingerprints to carry out the authentication followed by the transmitter identification. We provided closed-form expressions for the error probabilities (i.e., the performance) of most of the hypothesis tests, which were then verified by extensive simulation results.

This work opens up many interesting possibilities for future work. For example, when the Eve and/or Alice nodes are mobile, a Bayesian filtering framework (such as [30]) could be employed to track the motion of each mobile user to keep up with the need of obtaining the updated ground truth periodically. Additionally, a more general scenario whereby multiple Eve nodes (with the exact count of Eve nodes not known a priori) are present need to be studied. Finally, adapting the proposed method to more complex scenarios, e.g., multipath propagation, colored noise, reverberation etc., is yet another promising direction of research.

REFERENCES

- [1] I. F. Akyildiz, D. Pompili, and T. Melodia, "Underwater acoustic sensor networks: research challenges," *Ad hoc networks*, vol. 3, no. 3, pp. 257–279, 2005.
- [2] E. Felemban, F. K. Shaikh, U. M. Qureshi, A. A. Sheikh, and S. B. Qaisar, "Underwater sensor network applications: A comprehensive survey," *Int. J. Distrib. Sen. Netw.*, vol. 2015, pp. 5:5–5:5, Jan. 2016. [Online]. Available: <https://doi.org/10.1155/2015/896832>
- [3] W. Chen, H. Yu, Q. Guan, F. Ji, and F. Chen, "Reliable and opportunistic transmissions for underwater acoustic networks," *IEEE Network*, pp. 1–6, 2018.
- [4] Y. Liu, H. H. Chen, and L. Wang, "Physical layer security for next generation wireless networks: Theories, technologies, and challenges," *IEEE Communications Surveys Tutorials*, vol. 19, no. 1, pp. 347–376, Firstquarter 2017.
- [5] X. Wang, P. Hao, and L. Hanzo, "Physical-layer authentication for wireless security enhancement: current challenges and future developments," *IEEE Communications Magazine*, vol. 54, no. 6, pp. 152–158, June 2016.
- [6] G. Han, J. Jiang, N. Sun, and L. Shu, "Secure communication for underwater acoustic sensor networks," *IEEE communications magazine*, vol. 53, no. 8, pp. 54–60, 2015.
- [7] M. C. Domingo, "Securing underwater wireless communication networks," *IEEE Wireless Communications*, vol. 18, no. 1, pp. 22–28, February 2011.
- [8] Y. Cong, G. Yang, Z. Wei, and W. Zhou, "Security in underwater sensor network," in *2010 International Conference on Communications and Mobile Computing*, vol. 1, April 2010, pp. 162–168.
- [9] C. Lal, R. Petroccia, K. Pelekanakis, M. Conti, and J. Alves, "Toward the development of secure underwater acoustic networks," *IEEE Journal of Oceanic Engineering*, vol. 42, no. 4, pp. 1075–1087, Oct 2017.
- [10] G. Dini and A. L. Duca, "A cryptographic suite for underwater cooperative applications," in *2011 IEEE Symposium on Computers and Communications (ISCC)*, June 2011, pp. 870–875.
- [11] —, "Seflood: A secure network discovery protocol for underwater acoustic networks," in *2011 IEEE Symposium on Computers and Communications (ISCC)*, June 2011, pp. 636–638.
- [12] G. Ateniese, A. Caposelle, P. Gjanci, C. Petrioli, and D. Spaccini, "SecFUN: Security framework for underwater acoustic sensor networks," in *OCEANS 2015 - Genova*, May 2015, pp. 1–9.
- [13] M. Goetz, S. Azad, P. Casari, I. Nissen, and M. Zorzi, "Jamming-resistant multi-path routing for reliable intruder detection in underwater networks," in *Proceedings of the Sixth ACM International Workshop on Underwater Networks*. ACM, 2011, p. 10.
- [14] M. Zuba, Z. Shi, Z. Peng, J.-H. Cui, and S. Zhou, "Vulnerabilities of underwater acoustic networks to denial-of-service jamming attacks," *Security and Communication Networks*, vol. 8, no. 16, pp. 2635–2645, 2015.
- [15] L. Xiao, Q. Li, T. Chen, E. Cheng, and H. Dai, "Jamming games in underwater sensor networks with reinforcement learning," in *2015 IEEE Global Communications Conference (GLOBECOM)*, Dec 2015, pp. 1–6.
- [16] Q. Wang, H.-N. Dai, X. Li, H. Wang, and H. Xiao, "On modeling eavesdropping attacks in underwater acoustic sensor networks," *Sensors*, vol. 16, no. 5, 2016. [Online]. Available: <http://www.mdpi.com/1424-8220/16/5/721>
- [17] Y. Huang, P. Xiao, S. Zhou, and Z. Shi, "A half-duplex self-protection jamming approach for improving secrecy of block transmissions in underwater acoustic channels," *IEEE Sensors Journal*, vol. 16, no. 11, pp. 4100–4109, June 2016.
- [18] Y. Liu, J. Jing, and J. Yang, "Secure underwater acoustic communication based on a robust key generation scheme," in *2008 9th International Conference on Signal Processing*, Oct 2008, pp. 1838–1841.
- [19] Y. Huang, S. Zhou, Z. Shi, and L. Lai, "Channel frequency response-based secret key generation in underwater acoustic systems," *IEEE Transactions on Wireless Communications*, vol. 15, no. 9, pp. 5875–5888, Sept 2016.
- [20] M. Xu and L. Liu, "Sensevault: A three-tier framework for securing mobile underwater sensor networks," *IEEE Transactions on Mobile Computing*, pp. 1–1, 2018.
- [21] E. Felemban, "Advanced border intrusion detection and surveillance using wireless sensor network technology," *International Journal of Communications, Network and System Sciences*, vol. 6, no. 05, p. 251, 2013.
- [22] M. Stojanovic, "Recent advances in high-speed underwater acoustic communications," *IEEE Journal of Oceanic Engineering*, vol. 21, no. 2, pp. 125–136, Apr 1996.
- [23] D. B. Kilfoyle and A. B. Baggeroer, "The state of the art in underwater acoustic telemetry," *IEEE Journal of Oceanic Engineering*, vol. 25, no. 1, pp. 4–27, Jan 2000.
- [24] C. R. Berger, W. Chen, S. Zhou, and J. Huang, "A simple and effective noise whitening method for underwater acoustic orthogonal frequency division multiplexing," *The Journal of the Acoustical Society of America*, vol. 127, no. 4, pp. 2358–2367, 2010.
- [25] M. Erol-Kantarci, H. T. Mouftah, and S. Oktug, "A survey of architectures and localization techniques for underwater acoustic sensor networks," *IEEE Communications Surveys Tutorials*, vol. 13, no. 3, pp. 487–502, Third 2011.
- [26] B. Liu, H. Chen, Z. Zhong, and H. V. Poor, "Asymmetrical round trip based synchronization-free localization in large-scale underwater sensor networks," *IEEE Transactions on Wireless Communications*, vol. 9, no. 11, pp. 3532–3542, November 2010.
- [27] H.-P. Tan, R. Diamant, W. K. Seah, and M. Waldmeyer, "A survey of techniques and challenges in underwater localization," *Ocean Engineering*, vol. 38, no. 14, pp. 1663–1676, 2011.
- [28] T. Li and A. Nehorai, "Maximum likelihood direction-of-arrival estimation of underwater acoustic signals containing sinusoidal and random components," *IEEE Transactions on Signal Processing*, vol. 59, no. 11, pp. 5302–5314, Nov 2011.
- [29] G. P. Hancke and M. G. Kuhn, "An RFID distance bounding protocol," in *First International Conference on Security and Privacy for Emerging Areas in Communications Networks (SECURECOMM'05)*, Sept 2005, pp. 67–73.
- [30] M. M. U. Rahman, A. Yasmeen, and J. Gross, "PHY layer authentication via drifting oscillators," in *2014 IEEE Global Communications Conference*, Dec 2014, pp. 716–721.
- [31] Q. Yan and R. S. Blum, "Distributed signal detection under the Neyman-Pearson criterion," *IEEE Transactions on Information Theory*, vol. 47, no. 4, pp. 1368–1377, May 2001.
- [32] S. Sendra, J. Lloret, J. M. Jimenez, and L. Parra, "Underwater acoustic modems," *IEEE Sensors Journal*, vol. 16, no. 11, pp. 4063–4071, June 2016.
- [33] A. Song, A. Abdi, M. Badiy, and P. Hursky, "Experimental demonstration of underwater acoustic communication by vector sensors," *IEEE Journal of Oceanic Engineering*, vol. 36, no. 3, pp. 454–461, July 2011.
- [34] L. Xiao, Q. Li, T. Chen, E. Cheng, and H. Dai, "The makai experiment: High-frequency acoustics," in *Eighth European Conference on Underwater Acoustics (2006)*, 2006.